applied sciences

MDPI

Communication

Study of Anisotropic Friction in Gears of Mechatronic Systems

Zuzana Ságová [1], Valerii Vasilevich Tarasov [2], Ivana Klačková [1,*], Alexander Ivanovich Korshunov [2] and Milan Sága [3]

[1] Department of Automation and Production Systems, Faculty of Mechanical Engineering, University of Žilina, Univerzitná 8215/1, 010 26 Žilina, Slovakia
[2] Federal State Budgetary Institution of Science, Udmurt Federal Research Center of the Ural Branch of the Russian Academy of Sciences, Institute of Mechanics, Tatyany Baramzinoy Str., 34, 426067 Izhevsk, Russia
[3] Department of Applied Mechanics, Faculty of Mechanical Engineering, University of Žilina, Univerzitná 8215/1, 010 26 Žilina, Slovakia
* Correspondence: ivana.klackova@fstroj.uniza.sk; Tel.: +421-41-513-2812

Abstract: The article discusses the features of anisotropic friction, which can be used to refine the calculation of the efficiency in various friction and gear drives and transmissions in mechatronic systems. Friction processes are considered that determine the level of losses in friction and gear drives, which are complex and heterogeneous in a number of parameters: the contact patch, which depends on the quality of the contacting surfaces; the direction and intensity of sliding; load distribution, etc. A more complete understanding of the features of these processes requires the use of the concept of friction anisotropy, which is well known in tribology of mechatronics systems. The anisotropy effect is caused by the difference in the characteristics of the surface microgeometry and its physical and mechanical properties in relation to the direction of the tool marks remaining on the surface after machining. In the presence of anisotropic friction, in contrast to isotropic, the body moves at a certain angle to the direction of application of the perturbing (external) force. The situation is considered in detail within the framework of the tensor model of anisotropic friction. The model and methodological approaches considered in the paper to the estimation of friction anisotropy can be used to refine the calculations of friction losses. The aim of the work is to create mechanical and analytical models of frictional anisotropy for a more complete understanding of this phenomenon in relation to various friction pairs. This article may be of interest to specialists in the field of friction gears for solving problems related to improving the accuracy of calculations and quantifying friction losses.

Keywords: friction anisotropy; gear transmissions; friction; cylindrical surfaces; mechatronic systems

check for updates

Citation: Ságová, Z.; Tarasov, V.V.; Klačková, I.; Korshunov, A.I.; Sága, M. Study of Anisotropic Friction in Gears of Mechatronic Systems. *Appl. Sci.* **2022**, *12*, 11021. https://doi.org/10.3390/app122111021

Academic Editor: Alessandro Gasparetto

Received: 12 September 2022
Accepted: 28 October 2022
Published: 31 October 2022

1. Introduction

The processes of friction, which eventually define the level of losses during friction and gear transmissions used in manufacturing machines and robots [1], have complicated and non-uniform characters over the contact spot, depending on the quality of contact surfaces, on the direction and the intensity of sliding, the distribution of loading, etc. [2,3]. There are known works aiming to measure the coefficient of, e.g., the sliding friction of pairs of materials by means of a variable inclination tribometer [4].

For a deeper understanding of the peculiarities of these processes, it is useful to introduce the notion of friction anisotropy, widely known in tribology in mechatronics systems. The anisotropy effect [5] is caused by the difference in the microgeometry characteristics of the surface and its physio-mechanical properties, depending on the direction of tracks of a tool, left after mechanical processing of the surface, typical for cutting metals with a defined cutting edge, such as turning, drilling, milling, etc. [6–8]. Orthotropic friction (a special case of anisotropic friction) is usually known as the unequal frictional characteristic in two mutually perpendicular directions in the contact plane.

The aim of the work is to create a mechanical and analytical models of frictional anisotropy for a more complete understanding of this phenomenon in relation to various friction pairs.

2. The Phenomenon of Anisotropic Friction

In the common case in the presence of anisotropic friction, in contrast to isotropic friction, the body moves at a certain angle to the direction of the application of the disturbing (imposed) force. We shall consider this situation within the framework of the tensor model of the anisotropic friction [9,10].

At the orthotropic friction there are two directions on the surface of the body, when the isotropic body is moving in these directions it is possible to know the maximal and minimal values of friction coefficient, respectively. We place the axes X and Y in these directions (Figure 1) and designate the corresponding friction coefficients as K and k. Let $\vec{e}$ be the unit vector in the direction of the body motion, disposed at the angle α (the angle of motion) with the axis X. In order for the body, pressed to the surface by normal force N, to move in the direction $\vec{e}$, it is necessary to apply to the body certain active force P along the line OO_1 at the angle β (the angle of the application of the force) with the axis X [11–13]. The active force P compensates the originating friction force $F_{tr} = -P$. We shall designate $\theta = \alpha - \beta$ (the angle of deviation).

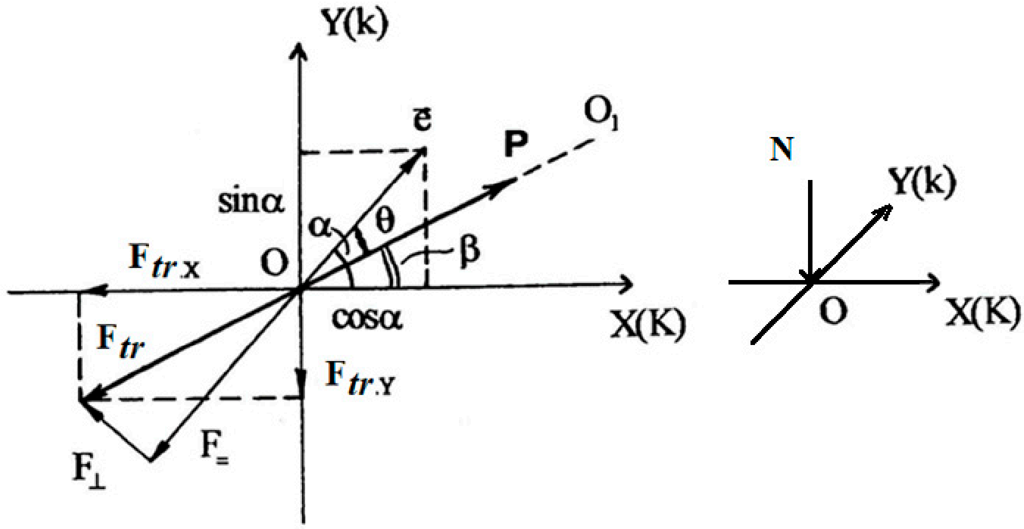

Figure 1. Scheme for the analysis of the process of anisotropic friction.

A normal force N is applied to a point O in a direction orthogonal to the drawing plane. Strength not shown.

In the accepted model of anisotropic friction for the constituents of the friction force along the axes X and Y we have:

$$\begin{cases} F_{trX} = -NK\cos\alpha \\ F_{trY} = -NK\sin\alpha \end{cases} \tag{1}$$

$$\text{Hence } tg = \frac{F_{trY}}{F_{trX}} = \frac{k}{K} tg\alpha, \tag{2}$$

and

$$F_{tr} = \sqrt{F_{trX}^2 + F_{trY}^2} = N\sqrt{K^2\cos^2\alpha + k^2\sin^2\alpha}\,. \tag{3}$$

The constituents of the friction force F_{tr}, projected in the direction of the $\vec{e}$ motion and on the direction normal to $\vec{e}$ [13–15], have the form

$$\begin{cases} F_{=} = F_{trX}\cos\alpha + F_{trY}\sin\alpha = -N(K\cos^2\alpha + k\sin^2\alpha) \\ F_{\perp} = -F_{trX}\sin\alpha + F_{trY}\cos\alpha = N(K-k)\cos\alpha\sin\alpha \end{cases} \quad (4)$$

For the angle of deviation θ we obtain

$$tg\theta = -\frac{F_{\perp}}{F_{-}} = \frac{(K-k)tg\alpha}{K + k\,tg^2\alpha}, \quad (5)$$

in this case, the angle θ lies within the limits from $-\theta_{max}$ to θ_{max}, where

$$tg\theta_{max} = 0.5\left|\sqrt{\frac{K}{k}} - \sqrt{\frac{k}{K}}\right|, 0 \le \theta_{max} < \frac{\pi}{2}. \quad (6)$$

In the first quadrant (at $0 < \alpha < \pi/2$) for the angle of deviation θ, we have $0 < \theta \le \theta_{max}$ if $K > k$ and $-\theta_{max} < \theta \le 0$ if $K < k$. In both cases the extreme value of the angle of deviation (θ_{max} or $-\theta_{max}$) is obtained at $tg\alpha = \sqrt{K/k}$. If $K = k$, then $\theta = 0$ for all the angles of motion α. Here at $k/K \Rightarrow 1$, friction degenerates into the isotropic one and at $k/K \Rightarrow 0$ it tends towards hypothetically absolute anisotropy.

In Figure 2, a mechanical simulation model is schematically presented for visual study of the peculiarities of friction and motion of the couple of bodies "anisotropic-isotropic surface". On the carrying plate of the model the supports of anisotropic friction are mounted as rolling bearings, having different resistance to the motion along to orthogonal directions [16–19]. Each support is given the angle of discrepancy of orientations among the supports φ_i (where $i = 1 \ldots n$; n = number of supports) with the direction of motion, it allows modeling different classes of indicatrix at unequal φ_i. The orientation of the model is rigidly fixed and its torque about its axis is compensated (the mode of plane-parallel motion).

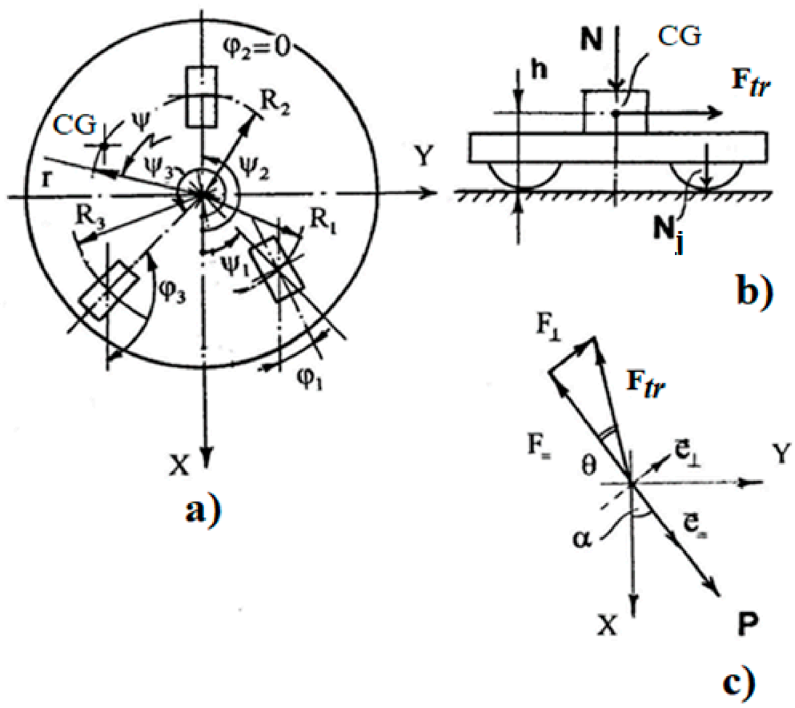

Figure 2. Calculation scheme of the mechanical model of anisotropic friction: (**a**) geometric parameters for calculation; (**b**) the scheme of application of forces; (**c**) power scheme, reduced to the center of gravity of the CG.

For the model, moving uniformly and linearly on three supports, the set of equilibrium equations has the following form:

$$\begin{cases} F_{=} = -\Sigma N_j\left[K\cos^2(\alpha-\varphi_j) + k\sin^2(\alpha-\varphi_j\right] \\ F_{\perp} = \Sigma N_j(K-k)\sin(\alpha-\varphi_j)\cos(\alpha-\varphi_j) \\ N = \Sigma N_j \\ -F_{\perp}h + Nr\sin(\Psi-\alpha) = \Sigma N_j R_j \sin(\Psi_j-\alpha) \\ -F_{=}h + Nr\cos(\Psi-\alpha) = \Sigma N_j R_j \cos(\Psi_j-\alpha) \end{cases}, \tag{7}$$

where N, N_j is general normal force and constituent normal force, respectively, per the j, which is the support; K, k are friction coefficients on a support in the orthogonal directions ($k << K$; R_j, r, which is a radius of disposition of the j, i.e., the support and the center of gravity of the model; Ψ_j, Ψ is the angle of disposition of the j, which is the support and the center of gravity of the model; φ_j is the angle of discrepancy of orientation of the j, which is the support with the direction of motion; and h is the height of motive force application [20,21].

The set of Equation (7) was realized through the programming language BASIC, and the integration Gauss method was used. The main graphic dependences of change of force and angular parameters of the model are represented in Figure 3 [22,23].

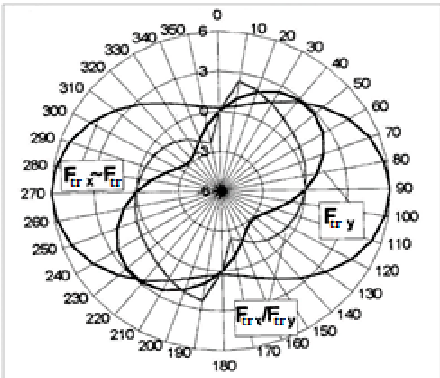

(**a**)

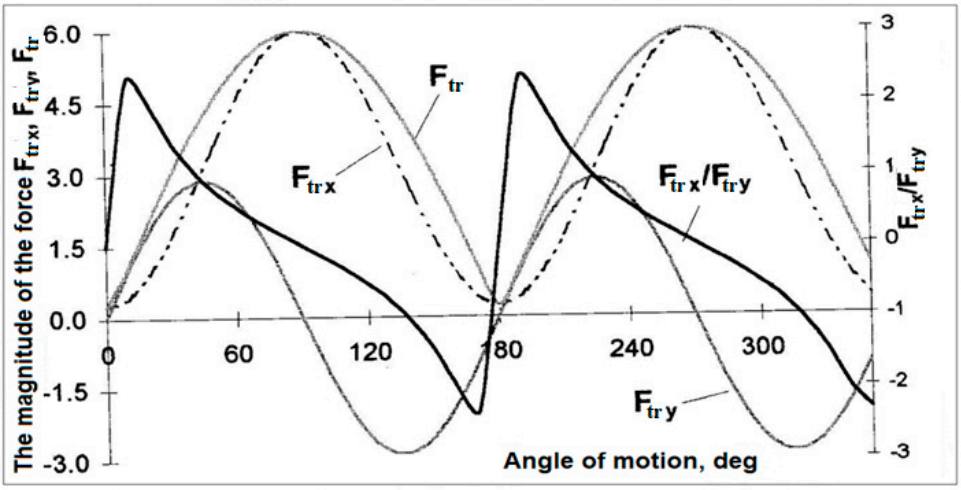

(**b**)

Figure 3. Change in the power characteristics of the mechanical model depending on the angle of motion in polar (**a**) and decretal (**b**) coordinates. Values F_{trX} and F_{trY} are projections of the friction force on the coordinate axes (Figure 1).

The changes of extreme values of the angular parameters of conjunction, depending on the factor k/K, are defined from the nomogram (Figure 4).

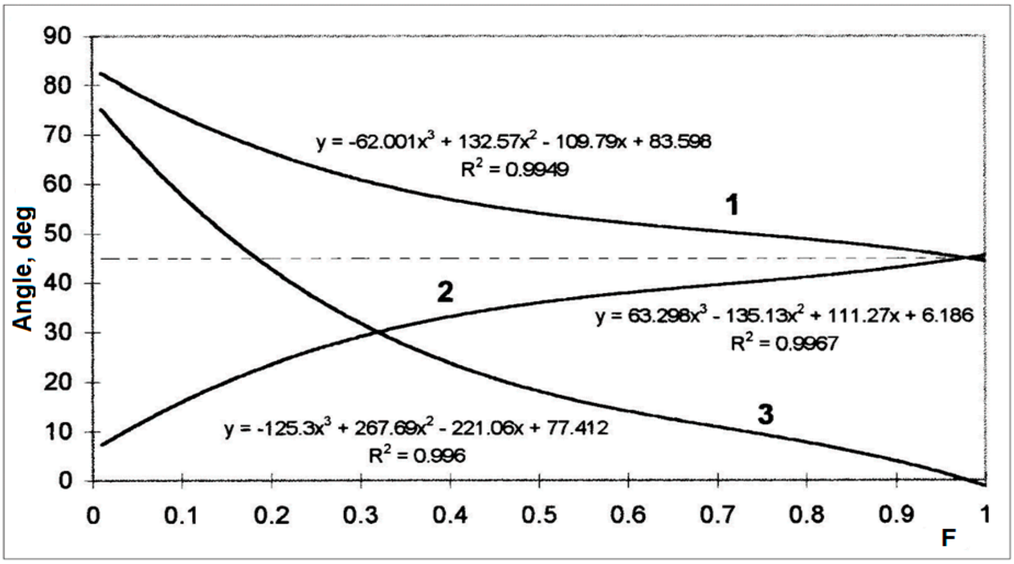

Figure 4. Nomogram for determining the maximum values of the angular parameters of the mechanical model from the friction anisotropy factor k/K.

In Figure 4, 1 is the angle of application of the driving force; 2 is angle of movement; and 3 is the slip angle.

For real pairs of friction $(k/K)_{max} > 0.6$, and technologically, it is difficult to achieve its further decrease [24–26]. The appearance of the materials with controlled friction characteristics allows the better use of the properties of anisotropic friction in various tribo-conjuctions. For friction transmissions (variators), which are kinematically similar to the simulation model (Figure 2), the anisotropy factor reaches the level of $(K_x/K_y)_{min} \approx 0.04$, and its influence becomes rather considerable; therefore, the revealed regularities can be used for designing the mechanisms with such transmissions and for computing their efficiency.

The comparison of the model representations according to Equation (7) with the experimental ones was carried out with the help of the mechanical model and special samples [27].

The experiments, conducted with the use of the mechanical model, have confirmed both the qualitative and quantitative correspondence of experimental and calculated results for the deviation angle θ and the force of resistance to the motion depending on the angle of motion α. The actual values of friction coefficients have been determined [28]. Thus, when the steel plate was used for the experiment, the following limiting coefficients were determined: $K_{max} = 0.123$ and $K_{min} = 0.05$ and $K_{min}/K_{max} = 0.041$, respectively.

The experiments with the use of special samples were carried out for the pairs "isotropic–anisotropic surface" without lubricant.

For the pair "steel 45–brass B62" under the loading Fn = 1.7 N, σ_K = 2.4 kPa, and the velocity V = 45–50 mm/min, the experimentally found friction coefficients were: $K_{max} = 0.25$ and $K_{min}/K_{max} = 0.816$. The deviation angle at different angles of the application of force changed within the range $\pm 3°$. In the preliminary experiments with the pairs "anisotropic–anisotropic surface", in some cases the deviation angle was up to 20°.

The comparison of experimental and calculated data shows qualitative coincidence of the model representations with the real ones in both the deviation angle (Figure 5) and the character of change of the motive force depending on the angle of motion. The exact approximating functions are the following:

- on the deviation angle $\theta = -0.25 + 2.60 \sin(2\alpha_{rad})$;
- on the motive force $F = 60.99 + 13.18 \sin^2(\alpha_{rad})$.

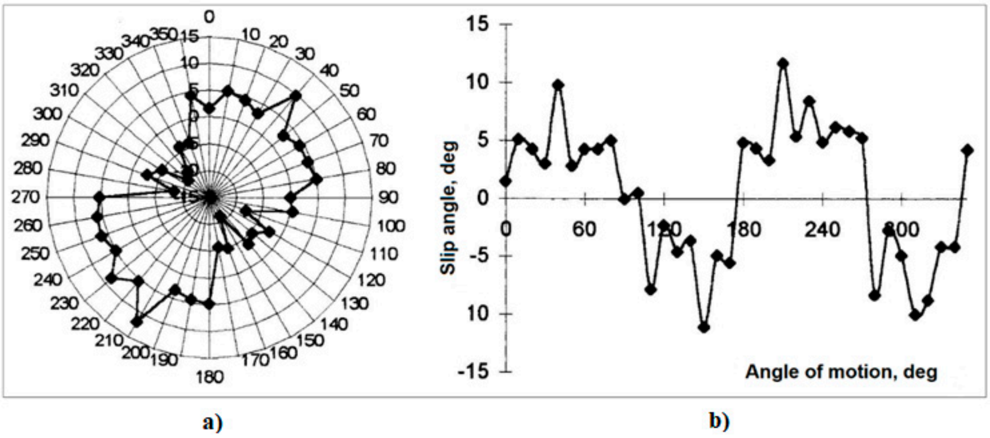

Figure 5. Change in the value of the slip angle from the angle of motion for full-scale samples in polar (**a**) and Cartesian (**b**) coordinates.

The quantitative coincidence of the model representations together with the real representations regarding the change of the components F_x and F_y of the friction force, depending on motion angle, has also been found. Experimental dependence is approximated by the curve of $F_x = 0.28 + 0.05 \sin^2(\alpha_{rad})$.

It has been shown that the increase of anisotropy factor leads to the increase of the deviation angle, which deviated in the range $\pm 12^\circ$ in the last case.

3. Estimation of Anisotropy of Friction Properties on Flat and Cylindrical Surfaces

For the estimation of anisotropy of the friction coefficient on the contact surfaces of the elements of friction and gear transmissions, the following technique can be used [28]: on the control surface, the indenter is moved along the circular trajectory and the components of the total vector of resistance forces are measured, these measurements are used for building up indicatrix. In tribometry, for the pairs "anisotropic–anisotropic body", which include the majority of elements of friction and gear transmissions, the motion of the indenter over the surface should be arranged in a way that the direction of anisotropy would never change its position when the moving along the given trajectory on the control body.

For the pair of samples from steel 45 with different roughness and with use of the indenter 2H, the friction coefficients $K_{max} = 0.162$ and $K_{min} = 0.134$ were obtained. The components of the friction force, acting upon the indenter, were determined in two perpendicular directions with the help of tensometric yoke. In the experiments the indenter was moved, while the mutual position of the selected axes of anisotropy was kept constant in a special device [29,30].

The accuracy of measurements in this technique would be better if the radius of the indenter itself were as small as possible and the radius of rotation of the indenter over the control surface were as large as possible. This technique can be used for flat surfaces or the surfaces with a small curvature; in the latter case, the indenter should be spring-loaded. In this way, it is possible to estimate the anisotropy of friction properties over the working surface, for instance, over the surface of teeth of gears or the non-cylindrical elements of friction variators [19–21].

The estimation of the anisotropy of friction on cylindrical surfaces should be considered more thoroughly.

Let the cylindrical body 1 with the anisotropy of frictional surface properties move along the axis **A–A** with the velocity V_c (Figure 6). The isotropic strip 2 is pressed to the surface of this body with force P in the area of the element **a–a** at an angle ξ; the isotropic strip only has the possibility of moving in the direction of the axis **B–B**. In this case, as the result of the contact interaction, the strip moves along the axis **B–B** with the velocity V_s.

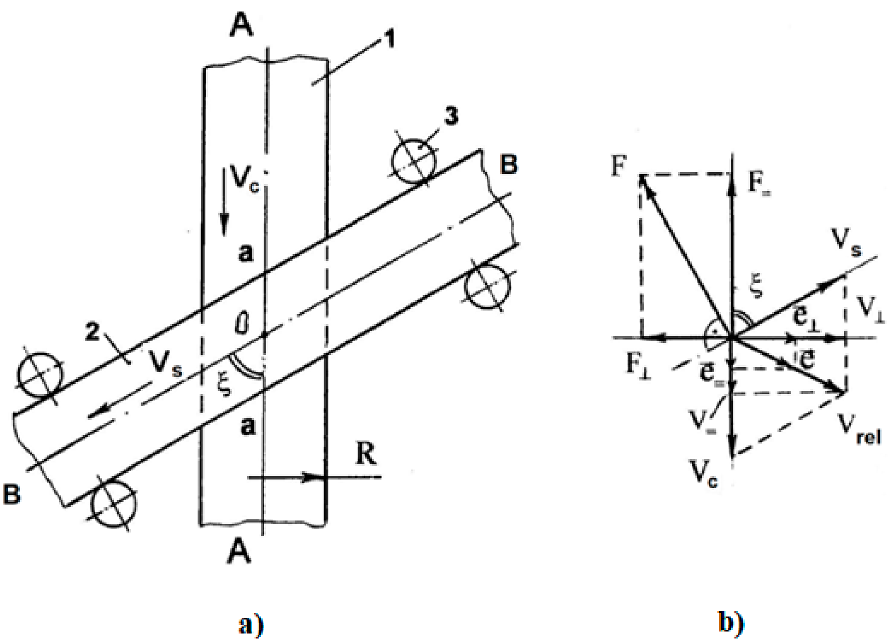

Figure 6. Calculation scheme of device for estimation of friction anisotropy on cylindrical surface (**a**) The design scheme of the device (Figure 7) and (**b**) the scheme of the application of forces.

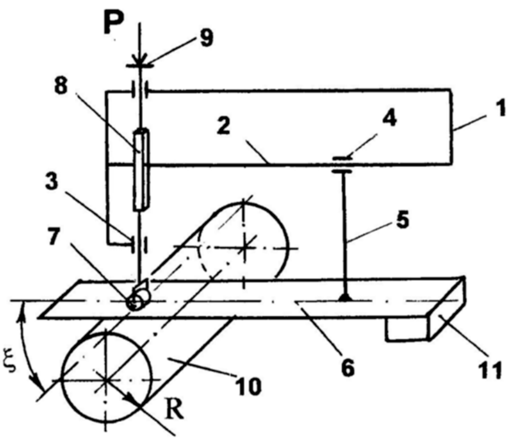

Figure 7. Kinematic scheme of device for the estimation of friction anisotropy on the cylindrical surface.

Following is the equilibrium equation for this case on the plane of tangency for the point **O**:

$$F_= \cos \xi - F_\perp \sin \xi = 0, \tag{8}$$

The values of $F_=$ and $F_\perp$ can be presented in the form

$$\begin{cases} F_= kNe_= \\ F_\perp = kNe_\perp \end{cases}, \tag{9}$$

where $e_=$ and $e_\perp$ are the projections of the unit vector e on the direction along the axis of the cylinder and perpendicular to it. They are determined as

$$\begin{cases} e_= = V_= / \sqrt{V_=^2 + V_\perp^2} \\ e_\perp = V_\perp / \sqrt{V_=^2 + V_\perp^2} \end{cases}, \tag{10}$$

Here, the velocities $V_{=}$ and $V_{\perp}$ are the constituents of the relative velocity V_{rel} of the motion of the cylinder and the strip [31], which can be found from the relationship:

$$\begin{cases} V_{=} = V_c - V_s \cos\xi, \\ V_{\perp} = -V_s \sin\xi, \end{cases} \tag{11}$$

Substituting (8) into (9), taking into account (10) and (11), after transformation we obtain:

$$\frac{K}{k} = [V_C / V_S \sin\xi, \mathrm{ctg}\xi]\mathrm{ctg}\xi\,, \tag{12}$$

Thus, there is the possibility of determining the anisotropy factor experimentally with the help of the measured velocities V_C and V_S.

With the rotation of the cylindrical body with the velocity ωR (R-cylinder radius), the component $V_{\perp}$ in the expression (13) should be calculated according to the formula

$$V_{\perp} = -V_S \sin\xi, \pm \omega R, \tag{13}$$

In expression (13), the plus (+) sign is used when there is a coincidence in directions of the vector of rotation velocity and the vector of the velocity of the motion of the strip [31], otherwise the minus (−) sign is taken. In this case, Formula (12) assumes the following form:

$$\frac{K}{k} = [(V_C / - V_S \sin\xi, \pm \omega R) - \mathrm{ctg}\xi]\mathrm{ctg}\xi\,, \tag{14}$$

In Figure 7, the device for the realization of the offered technique is shown.

The device in Figure 1 consists of a frame (1) with the axis (2) and guider (3). Regarding the axis (2) on the bearing block (4) through suspension (5), the standard strip (6) with isotropic roughness of the surface is attached; this strip is pressed with force P by the pressure roller (7) through the fork (8) to the control cylindrical sample (10) from the load center (9). To provide stability of motion, the iron rule (6) is fitted with a balance beam (11).

4. Conclusions

A simulation of a mechanical model has been developed in the form of a platform with oriented-controlled cylindrical rolling bearings, which makes it possible to simulate the effect of anisotropic friction when moving in different directions.

Based on the model and its mathematical representation, the relationships of the main characteristic parameters of tribosystems with anisotropic friction are obtained. Modeling the anisotropy of varying complexity (symmetries) is provided through the mutual misorientation of the supports.

The considered features of anisotropic friction can be used to improve the efficiency of the calculations of various friction and gear drives in mechatronic systems.

The proposed model and methodological approaches to estimating friction anisotropy can be used to improve the calculation of friction losses and develop control paths [31].

The authors suggest the continuation of experimental research in relation to gears in mechatronic systems.

The considered features of anisotropic friction, the proposed model, and methodological approaches to estimating the anisotropy of friction can be used for more accurate and reasonable calculations of the efficiency in various friction and gear drives and transmissions. This is also true for extremely loaded gears with a high coefficient of friction as presented by the authors in paper [32]. The application of the proposed method of calculation makes it possible to take into account the influence of a number of parameters that are omitted from the reasoning when conducting a significant number of calculations. The use of the tensor model of anisotropic friction has made it possible to refine a number of calculation formulas and provide a more accurate estimate.

Author Contributions: Conceptualization, V.V.T. and A.I.K.; methodology, Z.S. and I.K.; software, M.S.; validation, Z.S., I.K. and M.S.; formal analysis, V.V.T. and A.I.K.; investigation, M.S.; resources, I.K.; data curation, Z.S.; writing—original draft preparation, Z.S.; writing—review and editing, I.K.; visualization, I.K.; supervision, M.S.; project administration, I.K.; funding acquisition, I.K. All authors have read and agreed to the published version of the manuscript.

Funding: This work was supported through the project VEGA 1/0073/19. Project title: Computer modeling and development of algorithms for evaluating the reliability of composite structural elements produced by the additive technology based on Onyx for the purpose of optimal design and under the project KEGA 001ZU-4/2020. Project title: Implementing of additive technologies into the education process of engineers' study programs.

Conflicts of Interest: The authors declare no conflict of interest. The funders had no role in the design of the study; in the collection, analyses, or interpretation of data; in the writing of the manuscript, or in the decision to publish the results.

References

1. Peterka, J.; Nikitin, J.R.; Bozek, P. Diagnostics of automated technological devices. *MM Sci. J.* **2020**, *2020*, 4027–4034. [CrossRef]
2. Bragin, V.V.; Reshetov, D.N. *Designing of Cylindrical Gear Transmissions with High Tension*; Mashinostroenie: Moscow, Russia, 1991; p. 224.
3. Hebda, M.; Chichinadze, A.V. (Eds.) Techniques and means of tribotechnological testing. In *Tribotechnology Reference Book: V.3: Tribotechnology of Antifriction, Friction and Transmission Devices*; Mashinostroenie: Moscow, Russia, 1992; p. 730.
4. Kelemenova, T.; Dovica, M.; Bozek, P.; Kolarikova, I.; Benedik, O.; Virgala, I.; Prada, E.; Mikova, L.; Kot, T.; Kelemen, M. Specific Problems in Measurement of Coefficient of Friction Using Variable Incidence Tribometer. *Symmetry* **2020**, *12*, 1235. [CrossRef]
5. Opeyko, F.A. Experimental study of anisotropic friction. In *Collection of Scientific and Technical Works of MIMESH*; Soviet Science: Moscow, Russia, 1952; pp. 235–243.
6. Vopat, T.; Peterka, J.; Kovac, M.; Buransky, I. The Wear Measurement Process of Ball Nose End Mill in the Copy Milling Operations. In Proceedings of the 24th DAAAM International Symposium on Intelligent Manufacturing and Automation, Zadar, Croatia, 23–26 October 2013; Volume 69, pp. 1038–1047. [CrossRef]
7. Frankovský, P.; Delyová, I.; Trebuňová, M.; Čarák, P.; Kicko, M.; Kurylo, P. Motion Analysis of the Hydraulic Ladder. *Int. J. Appl. Mech. Eng.* **2019**, *24*, 230–240. [CrossRef]
8. Peterka, J.; Pokorny, P. Influence of the Lead Angle from the Vertical Axis Milling on Effective Radius of the Cutter. In Proceedings of the 7th International Congress of Precision Machining (ICPM 2013), Miskolc, Hungary, 3–5 October 2013; Volume 581, pp. 44–49.
9. Vopat, T.; Peterka, J.; Simna, V.; Kuruc, M. The Influence of Different Types of Copy Milling on the Surface Roughness and Tool Life of End Mills. In Proceedings of the 25th DAAAM International Symposium on Intelligent Manufacturing and Automation, Vienna, Austria, 26–29 November 2014.
10. Alexandrovich, A.I.; Vekshin, B.S.; Potapov, I.N. Tensor of friction coefficients of anisotropic surfaces. *Trenie Iznos* **1985**, *6*, 996–1004.
11. Tarasov, V.V. *Friction Anisotropy*; IM UB RAS: Izhevsk, Russia, 1998; p. 54.
12. Frankovsky, P.; Ostertag, O.; Ostertagova, E.; Trebuna, F.; Kostka, J.; Vyrostek, M. Experimental analysis of stress fields of rotating structural elements by means of reflection photoelasticity. *Appl. Opt.* **2017**, *56*, 3064–3070. [CrossRef]
13. Sharapin, Y.F. Elements of the theory of metal processing by pressure. *Metallurgizdat* **1961**, 208. (In Russian)
14. Kuric, I.; Klačková, I.; Domnina, K.; Stenchlák, V.; Sága, M., Jr. Implementation of Predictive Models in Industrial Machines with Proposed Automatic Adaptation Algorithm. *Appl. Sci.* **2022**, *12*, 1853. [CrossRef]
15. Tarasov, V.V. Method for Determination of Physico-Mechanical Properties of Material, Friction for the Most Part. A. s. USSR # 1388769, MKI G01N 19/02.
16. Saga, M.; Vasko, M.; Pechac, P. Chosen numerical algorithms for interval finite element analysis. *Procedia Eng.* **2014**, *96*, 400–409. [CrossRef]
17. Burduk, A.; Wiecek, D.; Tlach, V.; Ságová, Z.; Kochanska, J. Risk assessment of horizontal transport system in a copper mine. *Acta Montan. Slovaca* **2021**, *26*, 303–314. [CrossRef]
18. Kuric, I.; Tlach, V.; Císar, M.; Ságová, Z.; Zajačko, I. Examination of industrial robot performance parameters utilizing machine tool diagnostic methods. *Int. J. Adv. Robot. Syst.* **2020**, *17*, 1729881420905723. [CrossRef]
19. Sapietova, A.; Saga, M.; Novak, P.; Bednar, R.; Dizo, J. Design and Application of Multi-Software Platform for Solving of Mechanical Multi-Body System Problems. In Proceedings of the 9th International Conference on Mechatronics, Mechatronics: Recent Technological and Scientific Advances, Warsaw, Poland, 21–24 September 2011; pp. 345–354.
20. Maláková, S.; Puškár, M.; Frankovský, P.; Sivák, S.; Palko, M.; Palko, M. Meshing Stiffness—A Parameter Affecting the Emission of Gearboxes. *Appl. Sci.* **2020**, *10*, 8678. [CrossRef]
21. Muravev, V.V.; Muraveva, O.; Volkova, L.; Sága, M.; Ságová, Z. Measurement of Residual Stresses of Locomotive Wheel Treads During the Manufacturing Technological Cycle. *Manag. Syst. Prod. Eng.* **2019**, *27*, 236–241. [CrossRef]
22. Klarák, J.; Andok, R.; Hricko, J.; Klačková, I.; Tsai, H.-Y. Design of the Automated Calibration Process for an Experimental Laser Inspection Stand. *Sensors* **2022**, *22*, 5306. [CrossRef]

23. Segota, S.B.; Andelic, N.; Lorencin, I.; Saga, M.; Car, Z. Path planning optimization of six-degree-of-freedom robotic manipulators using evolutionary algorithms. *Int. J. Adv. Robot. Syst.* **2020**, *17*, 1729881420908076. [CrossRef]
24. Sága, M.; Blatnická, M.; Blatnický, M.; Dižo, J.; Gerlici, J. Research of the Fatigue Life of Welded Joints of High Strength Steel S960 QL Created Using Laser and Electron Beams. *Materials* **2020**, *13*, 2539. [CrossRef]
25. Puškár, M.; Jahnátek, A.; Kuric, I.; Kádárová, J.; Kopas, M.; Šoltésová, M. Complex analysis focused on influence of biodiesel and its mixture on regulated and unregulated emissions of motor vehicles with the aim to protect air quality and environment. *Air Qual. Atmos. Health* **2019**, *12*, 855–864. [CrossRef]
26. Kuric, I.; Klačková, I.; Nikitin, Y.R.; Zajačko, I.; Císar, M.; Tucki, K. Analysis of diagnostic methods and energy of production systems drives. *Processes* **2021**, *9*, 843. [CrossRef]
27. Ali, L.M.; Ali, Q.A.; Klačková, I.; Issa, H.A.; Yakimovich, B.A.; Kuvshimov, V.V. Developing a thermal design for steam power plants by using concentrating solar power technologies for a clean environment. *Acta Montan. Slovaca* **2021**, *26*, 773–783. [CrossRef]
28. Fiegel, A.; Klačková, I. Safety requirements for mining complexes controlled in automatic mode. *Acta Montan. Slovaca* **2020**, *25*, 417–426. [CrossRef]
29. Maláková, S.; Puškár, M.; Frankovský, P.; Sivák, S.; Harachová, D. Influence of the Shape of Gear Wheel Bodies in Marine Engines on the Gearing Deformation and Meshing Stiffness. *J. Mar. Sci. Eng.* **2021**, *9*, 1060. [CrossRef]
30. Handrik, M.; Kopas, P.; Baniari, V.; Vasko, M.; Saga, M. Analysis of stress and strain of fatigue specimens localised in the cross-sectional area of the gauge section testing on bi-axial fatigue machine loaded in the high-cycle fatigue region. In Proceedings of the XXI Polish-Slovak Scientific Conference Machine Modeling and Simulations MMS 2016, Hucisko, Poland, 6–8 September 2016; Volume 177, pp. 516–519. [CrossRef]
31. Abramov, I.V.; Abramov, A.I.; Nikitin, Y.; Sosnovich, E.; Božek, P.; Stollmann, V. Diagnostics of electrical drives. In Proceedings of the 18th International Conference on Electrical Drives and Power Electronics, Kosice, Slovakia, 21–23 September 2015. [CrossRef]
32. Virgala, I.; Kelemen, M.; Bozek, P.; Borovský, Z.; Hagara, M.; Prada, E.; Oscadal, P.; Varga, M. Investigation of snake robot locomotion possibilities in a pipe. *Symmetry* **2020**, *12*, 939. [CrossRef]